POLITECNICO
MILANO 1863

DIPARTIMENTO DI MECCANICA

mecc

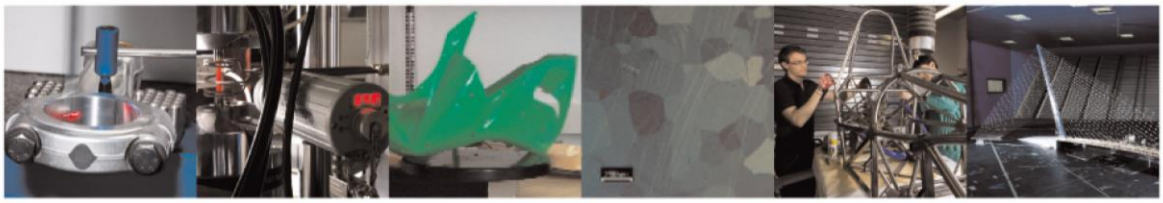

Characterizing Nanoparticle Release Patterns of Laser Powder Bed Fusion in Metal Additive Manufacturing: First Step Towards Mitigation Measures

Pernetti, Roberta; Galbusera, Francesco; Cattenone, Alberto; Bergamaschi, Enrico; Previtali, Barbara; Oddone, Enrico

This is a pre-copyedited, author-produced version of an article accepted for publication in Annals of Work Exposures and Health following peer review. The version of record Annals of Work Exposures and Health, Volume 67, Issue 2, March 2023, Pages 252–265, is available online at: https://doi.org/10.1093/annweh/wxac080.

Characterizing nano-particle release patterns of laser powder bed fusion in metal additive manufacturing: first step towards mitigation measures

Roberta Pernetti[a], *Francesco Galbusera*[b], *Alberto Cattenone*[c], *Enrico Bergamaschi*[d], *Barbara Previtali*[b], *Enrico Oddone*[a,d]

[a] Department of Public Health, Experimental and Forensic Medicine – University of Pavia, Pavia, Italy

[b] Department of Mechanical Engineering – Politecnico di Milano, Milano, Italy

[c] Università di Torino

[d]Unità Operativa Ospedaliera di Medicina del Lavoro – ICS Maugeri, Pavia, Italy

* Corresponding Author: Roberta Pernetti, Department of Public Health, Experimental and Forensic Medicine – University of Pavia, via Boezio 24, 27100 Pavia, Italy
roberta.pernetti@unipv.it +39 0382 593802

Abstract

Laser Powder Bed Fusion (L-PBF) is a well-known Additive Manufacturing (AM) technology with a wide range industrial application. Potential occupational exposures to metal nanoparticles (NP) as by-products could occur in these processes, and no cogent occupational exposure limits are available. To contribute to this assessment, a monitoring campaign for measuring the NP release pattern in two metal L-PBF facilities was carried out in two academic laboratories adopting L-PBF technology for research purposes. The monitored processes deal with two devices and feedstocks, namely stainless steel (AISI 316L), aluminium-silicon alloy (A357) and pure copper that are associated to different level of industrial maturity. Prolonged environmental and personal real-time monitoring of nanoparticle concentration and size were performed, temperature and relative humidity were also measured during environmental monitoring. The measurements reveal a controlled NP release of the monitored processes entailing an average reduced exposure of the operators during the whole working shift, in compliance with proposed limit values (20,000 n/cm3 for density >6,000 kg/m^3 or 40,000 N/cm^3 for density <6,000 kg/m^3). Nonetheless, the monitoring shows release events with an increase of NP concentration and a decrease of NP size in correspondence to several actions usually performed during warmup and cleaning, leading to exposures over 40-50,000 N/cm^3, for not negligible time interval especially during the manufacturing of pure copper powder. The results show that actions of the operators, boundary conditions (relative humidity), and set-up of the L-PBF device, have an impact on the amount of NP released and their size. Several release events (significant increase of NP concentration and decrease of NP size) are identified and associated to specific job task of the workers as well as building conditions. These results contribute to the definition of NP release benchmarks in AM processes and to provide information to improve the operational conditions of L-PBF processes as well as the safety guideline for the operators.

Keywords

Additive manufacturing, indoor air quality, metal nanoparticle exposure, occupational health

Highlights

Monitoring actual conditions and operative set-up of advanced procedures including interruptions and production problems

Real-time release assessment additive manufacturing systems

Adoption of alloys associated to different level of L-PBF technology maturity

1. Introduction

Additive Manufacturing (AM) is an emerging technology that allows to produce complex objects through the addition of subsequent layers of material according to digital control based on 3D models (ISO standard, 2019). Metal AM processes are based on an energy source used to melt the metal powders according to the object design, enabling to reduce the environmental impact of the production increasing the process sustainability (Niaki, Torabi, and Nonino, 2019; Böckin and Tillman, 2019). According to the ISO/ASTM 52900:2021 (ISO standard, 2021), one of the main categories is Powder Bed Fusion (PBF), where the feedstock is a metallic round powder, evenly distributed using a coating mechanism onto a substrate plate and selectively melted by a high energy source. When a laser beam is applied as energy source, the process is called Laser Powder Bed Fusion (L-PBF).

The high energy for melting the powder, whose initial diameter usually ranges from 15 to 63 μm according to the composition and application, entails the release of metal fine and nanoparticles (NP) as by-product of L-PBF processes (Kolb et al., 2017). Despite the laser melting occurs in a sealed camera, and the AM device is usually placed in a dedicated environment with mechanical ventilation, metal NP have been detected in proximity of the AM device (Jensen et al., 2020; Sousa, Arezes, and Silva, 2021). Moreover, the operators interact with the device for several activities e.g., handling powders, charging the tank, cleaning the components, and emptying the overflow container after the build job. These activities may lead to a potential exposure for metal particles and NP that may increase the risk of lung inflammation (Vallabani et al., 2022) and asthma for the AM operators (Duffin et al., 2007).

Further than the concentration, the aerodynamic diameter of generated particles represents one of the main factors affecting the likelihood of the exposure, since the size influences the percentage of deposition along the respiratory airway: the finest particles can reach the gas exchange zone (i.e., the bronchioles and alveoli) being also able at nanoscale to cross the air/blood barrier with an efficiency

inversely correlated to the particle size (Kreyling et al., 2014; Bengalli et al., 2017)), and present a more difficult disposal (Duffin et al., 2007). The particle size also influences the exposure pattern, affecting the deposition time and the persistence in the working environment (Kuijpers et al., 2017). NP are characterized by a slow sedimentation rate (Fonseca *et al.*, 2016; Mellin et al., 2016) and can be detected for several hours after the end of the building process (Shi et al., 2015), also depending on ventilation rate and relative humidity (Wang et al., 2017).

Previous reviews (Sousa, Arezes, and Silva, 2019; Chen et al., 2020) highlight only few studies investigating NP exposure in AM facilities through real-time on-field monitoring, pointing out the need to further characterize the release of NP as by-products, from physical, chemical and toxicological perspectives (Wang et al., 2021).

The current references developed by ACGIH (American Conference of Governmental Industrial Hygienists, 2021), OSHA (Occupational Safety and Health Administration, 2020) and NIOSH (National Institute of Occupational Safety and Health, 2007) for metal exposure are based on traditional technologies (such as welding, grinding, melting) and prescribe mass evaluation. Therefore, these limits do not provide an effective assessment of the release in terms of size and concentration and proper hazard evaluation. A recent study reported a case in one AM facility where the metal concentrations comply the limits assessed through gravimetric evaluation. Nevertheless, further analyses on AM operators' urine presented a concentration of chromium, cobalt, and nickel 20-30% higher than the administrative personnel of the company (Ljunggren et al., 2019), highlighting an exposure.

There is the need of systematic studies on different metal AM settings in order to characterize particle release and to provide a structured knowledge about their features, distribution over time and space, in order to support the definition of benchmarks and standardised exposure limits

(Pieter Van Broekhuize et al., 2012). In this regard, the authors performed a preliminary measurement campaign based on standard gravimetric analysis for evaluating the respirable and inhalable dust in the monitored sites (Oddone et al., 2021). The results of the gravimetric analysis showed concentrations 5-100 times lower than the TLVs for the analysed metals, while the results of the particle counting (0.3-25 μm) were in line with (Ljunggren et al., 2019), that also detected the release of nanoparticles. Therefore, aim of this study is to complete the characterization of AM emissions provided by (Oddone et al., 2021) by focusing on of nanoparticles, whose monitoring and quantification is reported only in few studies, in order to identify the pattern of release and the activities entailing an increase of the concentration as well as a reduction of the particle size.

The relevance of this work lays in the presentation of data from prolonged monitoring of operative conditions of AM processes, including deviations from the standard procedures and malfunctioning. The monitored processes apply three alloys associated to a different level of maturity in AM application: i) stainless steel (AISI 316L) has been widely investigated and it is commonly adopted in industrial AM settings with standard process parameters, ii) aluminium based alloy (A357) that presents several potential applications and it is in advanced research phase for the definition of proven process parameters, iii) pure copper (Cu), whose application in AM is still in research phase for defining effective process parameters.

2. Materials and methods

2.1. Main features of AM sites

The two monitored devices in Politecnico of Milano (POLIMI) and University of Pavia (UNIPV) are used for research on process optimization. Both systems are L-PBF architectures, entailing the addition of a series of powder layers ranging from 20 to 60 μm of thickness, depending on the

processed material, on the building plate that is melted by the laser beam according to the job design. The processes of the printer 3D-NT LLA150 (Prima Additive, Torino, Italy) were analysed in POLIMI, while the processes with the printer Renishaw AM250 (Renishaw, Stone, UK) were monitored in UNIPV. The first machine is an open L-PBF system, with the ability to operate the laser source in different modes (pulsed and continuous wave emission) and to process new and non-commercial powders while varying process parameters, scanning strategy and inert gas type. The second system is a more rigid and consolidated system, processing standard powders according to the manufacturer's specifications.

Prior to manufacturing, the build chamber is filled with argon and oxygen content is maintained at 2300 ppm for POLIMI machine and below 1000 ppm for UNIPV machine (i.e., inertization). The excess powder is funnelled in the overflow container and removed during cleaning operation for being sieved and re-used in further processes.

The two sites present different boundary conditions. POLIMI presents an open-space laboratory with separated metal boxes (surface 5.4 m^2) for each AM device. The boxes are conditioned and ventilated by a central mechanical system that ensure a complete air change rate of the room every 4 minutes (c.a. 0.25 vol/min). The device in UNIPV is installed in a dedicated room (surface 8.5 m^2) with local climatization system and natural ventilation.

2.2. Monitoring approach

The monitoring campaign focused on the measurement of real-time nanoparticle concentrations released during the whole building processes. The monitoring was performed through one Miniature Diffusion Size Classifier (DiSCMini – TESTO), based on the measure of the induced unipolar charging of the particles flowing through two subsequent electrometer stages. It allowed to quantify the particle concentration in the sampled air [n/cm^3] and the average particle size [nm] within the range 10-300 nm (Fierz et al., 2011). Both environmental monitoring (ENV), by positioning the sensors next to the build chamber door and personal monitoring (PERS), sampling in the breathing

zone of the operators were conducted. Table 1 summarizes the chemical composition and properties of the powder feedstocks implemented as well as the process data:

- z (μm) - layer thickness.
- v (mm/s) - scan speed of the laser beam.
- E (J/mm^3 - volumetric energy density transmitted by the laser beam during processing. It depends on the process parameters used during L-PBF. It is used to compare different energy input conditions and to predict the densification of the as-built samples.
- m' - percentage of material undergoing vaporization during processes. It is estimated with the lumped capacity method described by Steen in (Steen and Mazumder, 2010) and it depends on the process parameters as well as the thermophysical properties of the powder feedstocks. More detailed information about the model and its inputs are shown in Table SM3 and SM4 (supplementary materials).

Table 1. AM systems, compositions of the feedstocks

Nominal chemical composition, density (ρ) and granulometry (D).												
wt.%	**Al**	**C**	**Cr**	**Cu**	**Fe**	**Mg**	**Mn**	**Mo**	**Ni**	**Si**	**ρ (g/cm^3)**	**D (μm)**
AISI 316L	-	0-0.03	16-18	-	61.9-72	-	0-2	2-3	10-14	0-1	8	15-45
A357	92.4	-	-	-	-	0.6	-	-	-	7	2.67	15-45
Pure Cu	-	-	-	100	-	-	-	-	-	-	8.93	20-63
Processes set-up data												
Process		**Feedstock**		**z (μm)**		**v (mm/s)**		**P (W)**		**E (J/mm^3)**		**m' (%)**
PV_316L_ENV		AISI 316L		50		1000		200 CW		57		0.12
PV_316L_PER		AISI 316L		50		1000		200 CW		57		
MI_A357_PERS		A357		25		1000		200 CW		89		0.22
MI_A357_ENV		A357		25		1000		200 CW		89		
MI_Cu_ENV		Pure copper		25		355		250 CW		2067		0.68
MI_Cu_PERS		Pure copper		25		355		250 CW		2067		
MI_Cu_ENV_2		Pure copper		25		355		250 CW		2067		

The environmental monitoring dealt with the whole manufacturing process that, for the purposes of this work, is divided in four phases summarized in Figure 1:

- *Warmup (open chamber)*: preliminary activities for launching the build job: preparation of the building chamber, calibration of the recoater, charging raw powders, device general settings;

- *Building (closed chamber)*: including inertization and de-inertization operations and the process entailing the use of laser for building the object;
- *Pause (closed chamber)*: time intervals from the end of the build job to the beginning of cleaning or after cleaning;
- *Cleaning (open chamber)*: removal of the substrate, removal of the built object, cleaning of the build volume with brushes and vacuum to remove small quantities of powder deposited in the mechanic gaps, emptying of the overflow container and cleaning of the filters.

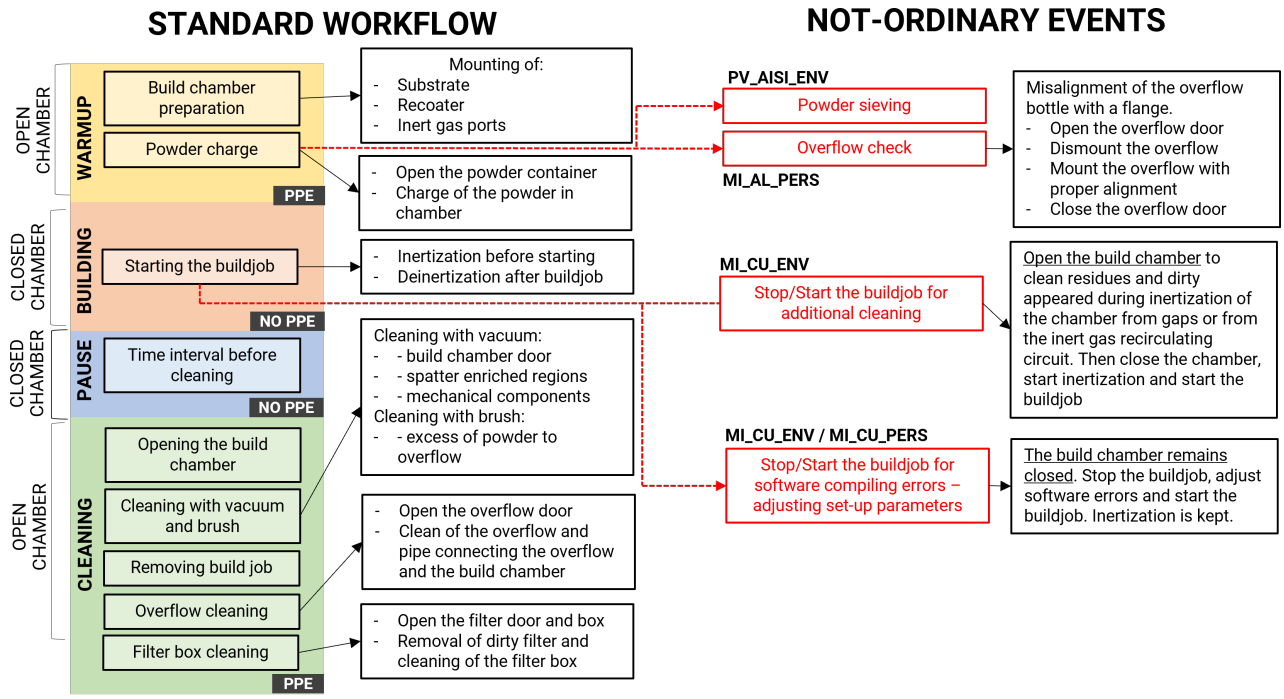

Figure 1. Flowchart of a standard LPBF process and job tasks with the identification of not-ordinary events during the monitoring campaign. PPE/NO PPE indicate respectively that the operators wear and do not wear personal protection equipment

The personal monitoring dealt with the phases with a direct interaction between the operators and the manufacturing system, namely Warm-up and Cleaning. Coupled with the environmental monitoring of NP, a datalogger 174-H (Testo) was adopted for measuring the air temperature (accuracy ± 0.5 °C) and relative humidity (accuracy ± 3%) in the 3D system dedicated-box.

The environmental background of airborne NP was estimated by measuring the concentration of NP in proximity for a time interval of 5' and in correspondence to the desks where the operators use to work during the building process.

2.3. Statistical analysis

The normal distribution of variables (nanoparticle number and size, air temperature and relative humidity) was checked by Shapiro-Wilk test. Since these continuous variables are not normally distributed, they were described in terms of median and interquartile range. Statistical differences between median values of considered variables were tested by Kruskall-Wallis method. Correlations between number and size of NP, air temperature and relative humidity were carried out using regression coefficients (β) calculated according to quantile regression method. The significance level was set at alpha 0.01 (statistical significance at $p<0.01$), and all tests were two tailed. The analyses were conducted with STATA software (version 14; Stata Corporation, College Station, TX, USA, 2015).

3. **Results**

The data were collected through different monitoring sessions from July 2021 to January 2022, with a focus on sample days representing the usual operation in an AM facility. Table 1 reports the nominal chemical compositions, density and granulometry of the powders processed during the experimental activity. In each building phase, the samples were built upon proper substrates, whose material was a stainless steel for AISI316L and pure Cu powders and aluminium for A357. Table 2 shows an overview of the six monitored processes in terms of monitoring types and phases with their correspondent lengths.

Table 2. Overview of the monitored processes in terms of monitoring type and phases and warm-up, building and cleaning lengths.

Process	Location	Date	Type	Phases	Duration of the monitored phases		
					Warm-up	Building	Cleaning
PV_316L_ENV	PV	07/21	Environmental	Whole process	55'	30 h	2h + 3h 40'
PV_316L_PER		12/21	Personal	Warmup-cleaning	1h 28'	-	40'
MI_A357_PERS	POLIMI	11/21	Personal	Warmup-cleaning	40'	-	2h 20'

MI_A357_ENV	11/21	Environmental	Whole process	50'	3h 52'	1h 08'
MI_Cu_ENV	12/21	Environmental	Whole process	2h 39'	5 h	1h 31' + 1 h 34'
MI_Cu_PERS	01/22	Personal	Warmup-cleaning	2h 4’	-	2h 54’
MI_Cu_ENV_2	01/22	Environmental	Building	-	10 h	-

The box plot charts of the environmental monitoring (Figure 2) highlight a general increase of the nanoparticle concentration respect to the background (values in dotted line). The process presenting the higher release is MI_A357_ENV, with an average +36% of concentration respect to the background, while MI_Cu_ENV showed a +20% and PV_316L_ENV a +9%m, taking in account the average values of all the monitored phases. The highest increases respect to the background were collected in case of adoption as feedstock of pure Cu powder (+ 60%) and A357(+104%), corresponding to an enhance of the particle concentration respectively of + 3120 n/cm^3 and 5540 n/cm^3(for more detailed data please refer to Table SM1 and SM2 of supplementary materials). This increase occurs during the building phase, when the build chamber is sealed and filled by argon and its recirculation system should filter the powders.

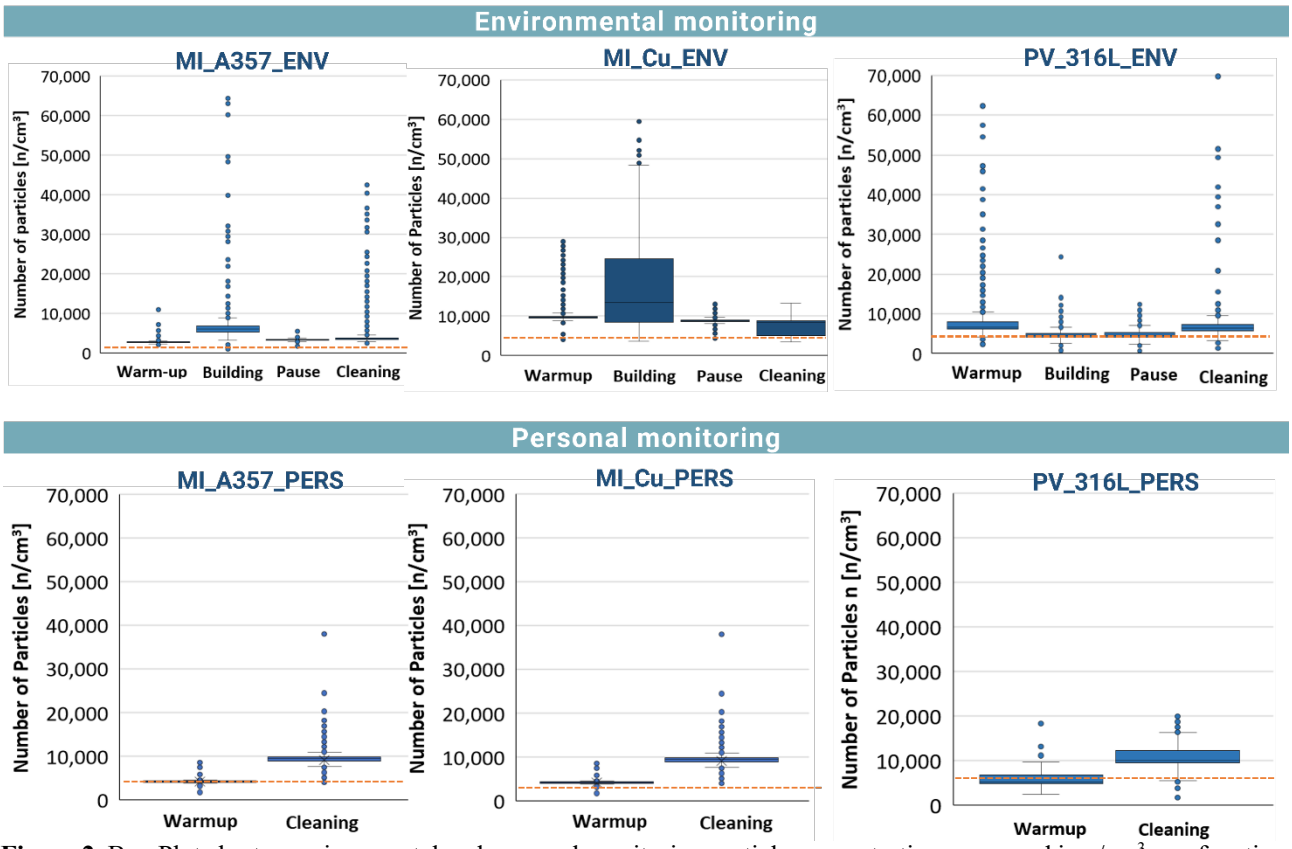

Figure 2. Box Plot chart – environmental and personal monitoring particle concentration expressed in n/cm^3 as a function of the phase (in dotted line the background concentration)

The results show a different pattern of release for the powders. MI_Cu_ENV presents large interquartile ranges representing frequent variations, mainly increases, respect to the average concentration and a more constant release during the warmup and building. MI_A357_ENV and PV_316L_ENV show a comparable pattern of release with reduced interquartile ranges, laying within concentrations lower than 10,000 n/cm^3 (that is not exceeded by the whiskers as well). On the other hand, several values above the whiskers are observed meaning that MI_A357_ENV and PV_316L_ENV present in general a reduced release during the process phases that is coupled with significant peaks corresponding to release events.

Figure 2 also shows the boxplot for personal monitoring (warmup and cleaning), presenting the concentrations below 70,000 n/cm^3 for the readability of the charts. Only few peaks above 70,000 n/cm^3 are not included in this representation, namely 7 points during the warmup for MI_A357_PERS and 2 points during the cleaning phase for MI_Cu_PERS. PV_316L_PERS does not present any peaks above 20,000 n/cm^3. MI_A357_PERS presents the higher fraction of measurements above the whiskers during warmup and cleaning because of the reduced density and high volatility of A357 alloy. More detailed results are presented in supplementary materials.

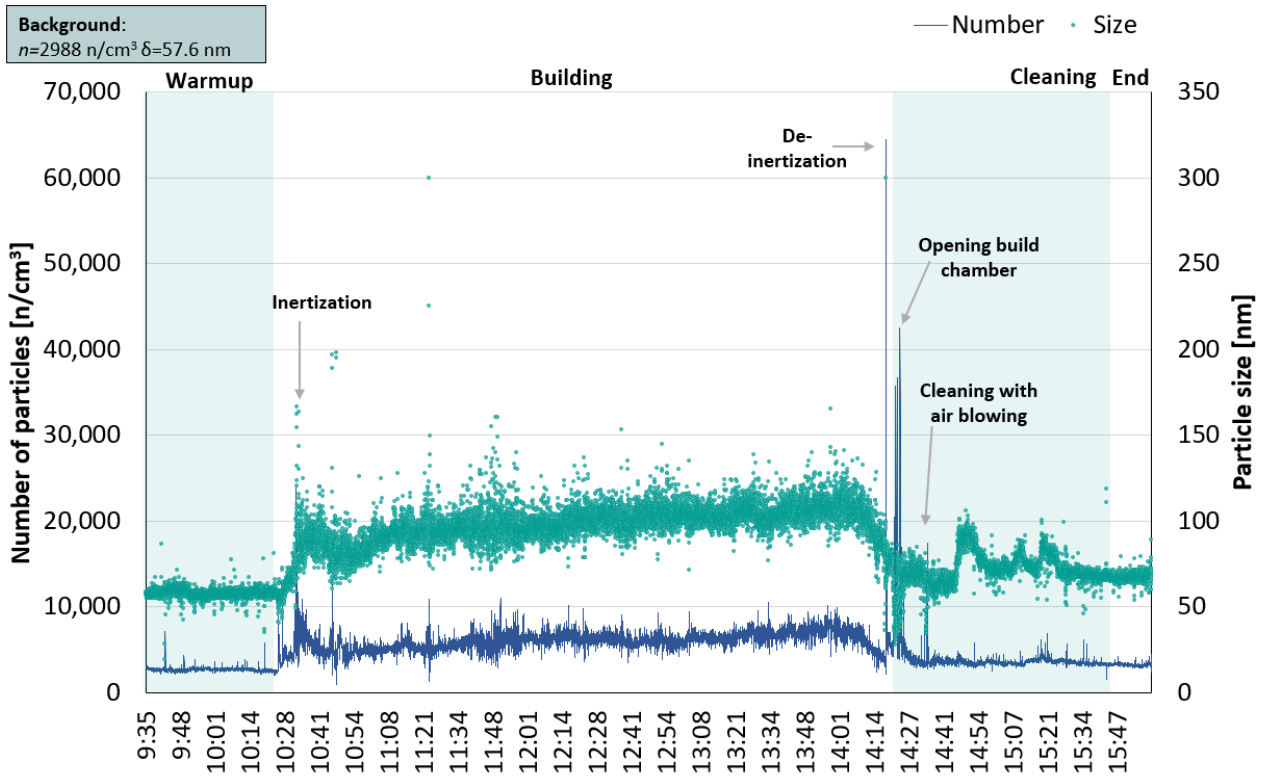

Figure 3. Real-time particle measurement - Environmental monitoring MI_A357_ENV – Number and size of the particles detected as a function of time and operation phase. Background measurements are displayed at the top left of the chart, confidence interval: number 2622-3354n/cm^3, size 49.3-65.9 nm.

Figure 3 shows the time course of the pattern for particles' concentration and size highlighting the job tasks corresponding to the release events as registered in the activity diary. MI_A357_ENV followed the standard process workflow and reveals a limited release (<10,000 n/cm^3 on average respect to the 2,988 n/cm^3 registered as background), with some significant peaks at the beginning (23,600 n/cm^3) and at the end of the manufacturing process (64,400 n/cm^3), respectively during the inertization and de-inertization of the build chamber, supposed to be closed and sealed during these operations. Another release event is associated to the beginning of cleaning operations, when the operator opens the build chamber, and when the printed job is cleaned by blowing air. It is possible to underline events with high increase of NP concentration (>30,000 n/cm^3), in correspondence to the opening of the build chamber. These peaks are associated to a reduction of the particle size (from average diameter of 75 nm to < 28 nm) meaning that during specific activities a significant release of NP with reduced size occurs. Further release events are pointed out by personal monitoring in

correspondence of the use of vacuum for cleaning the build chamber and the mechanisms for moving the building plate and when handling the filter for the argon recirculation.

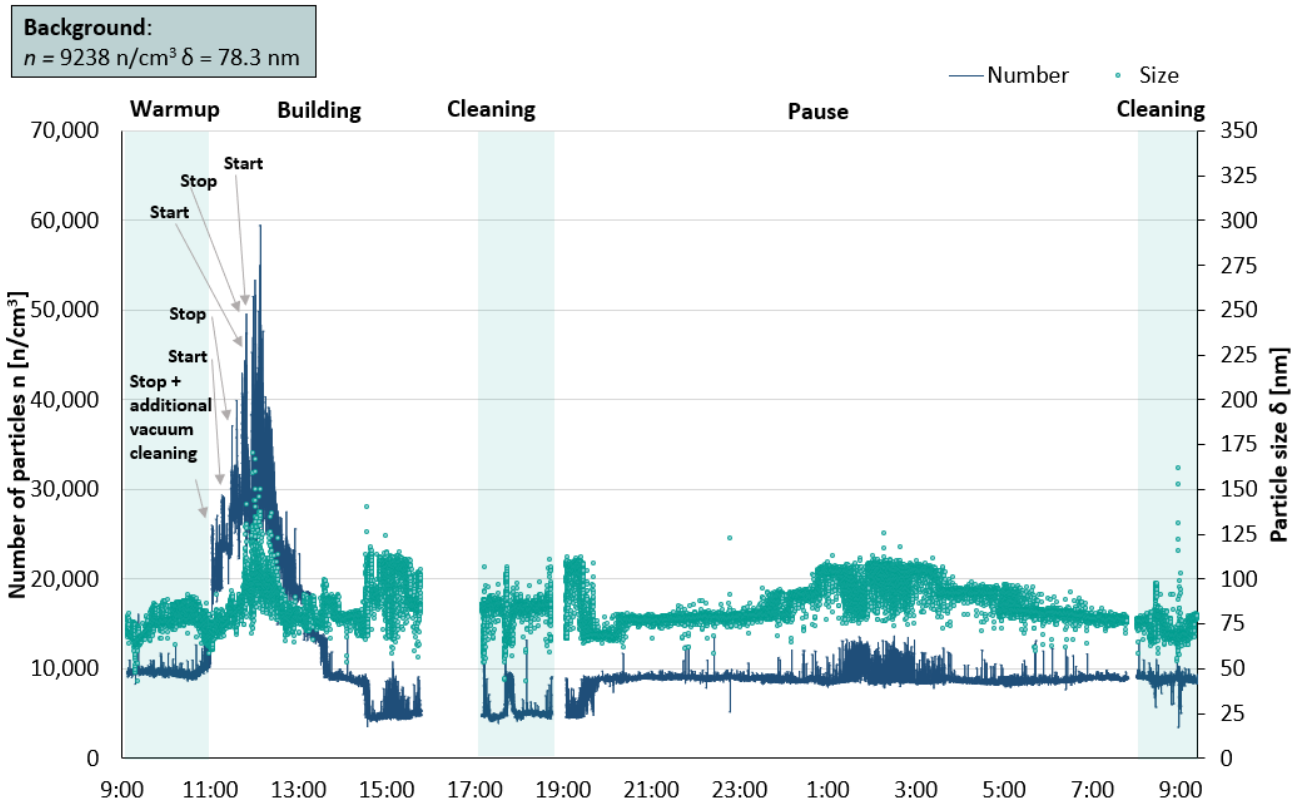

Figure 4. Real-time particle measurement - Environmental monitoring MI_Cu_ENV – whole process. Number and size of the particles detected as a function of time and operation phase. Background measurements are displayed at the top left of the chart, confidence interval: number 8627-9850 n/cm^3, size 66.8-89.8 nm.

The process MI_Cu_ENV (Figure 4) reveals a limited release during warmup and cleaning, with no significant peaks. Manufacturing phase entails a particle release from around 10,000 toward 59,500 n/cm^3, also associated to an increase of the particle diameter from 60 nm to 160 nm. This release interval occurred at the beginning of the building phase, from 11:20 to 12:55, in correspondence to a series of starts and stops of the building process for adjusting the set-up parameters (not-ordinary events, see Figure 1). The first one relates to an additional cleaning after the inertization for removing residues of previous build jobs with different powders (open chamber), while other release events deal with adjustments of process set-up by the operator (closed chamber).

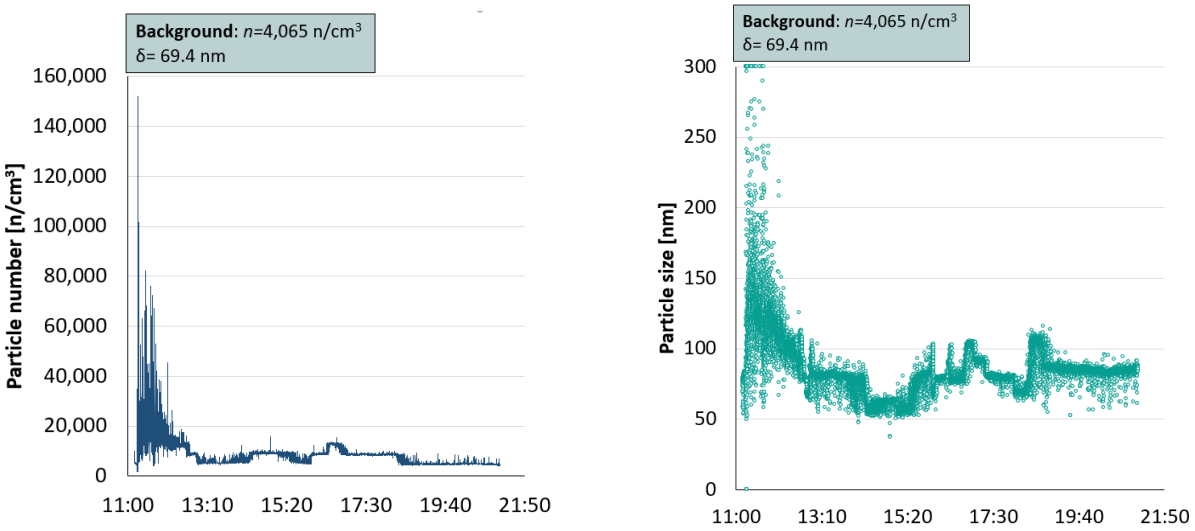

Figure 5. Real-time particle measurement - Environmental monitoring MI_Cu_ENV_2 – building phase. Number and size of the particles detected as a function of time. Background measurements are displayed at the top left of the chart, confidence interval: number 3876-4254n/cm^3, size 67.2-71.6 nm.

A comparable release pattern also occurred in an additional environmental monitoring performed during the building phase of MI_Cu_ENV_2 (Figure 5), at the beginning of building, from 11.05 to 12.05. During the build job, two starts and stops were performed to abort some samples owing to an unproper power delivery on the baseplate, potentially causing defects on the recoater system. In both processes, during these activities, some not-ordinary events occurred (see Figure 1) and the operators interacted with the AM device for adjusting the building setup and the build chamber remains sealed with the inertization kept as constant.

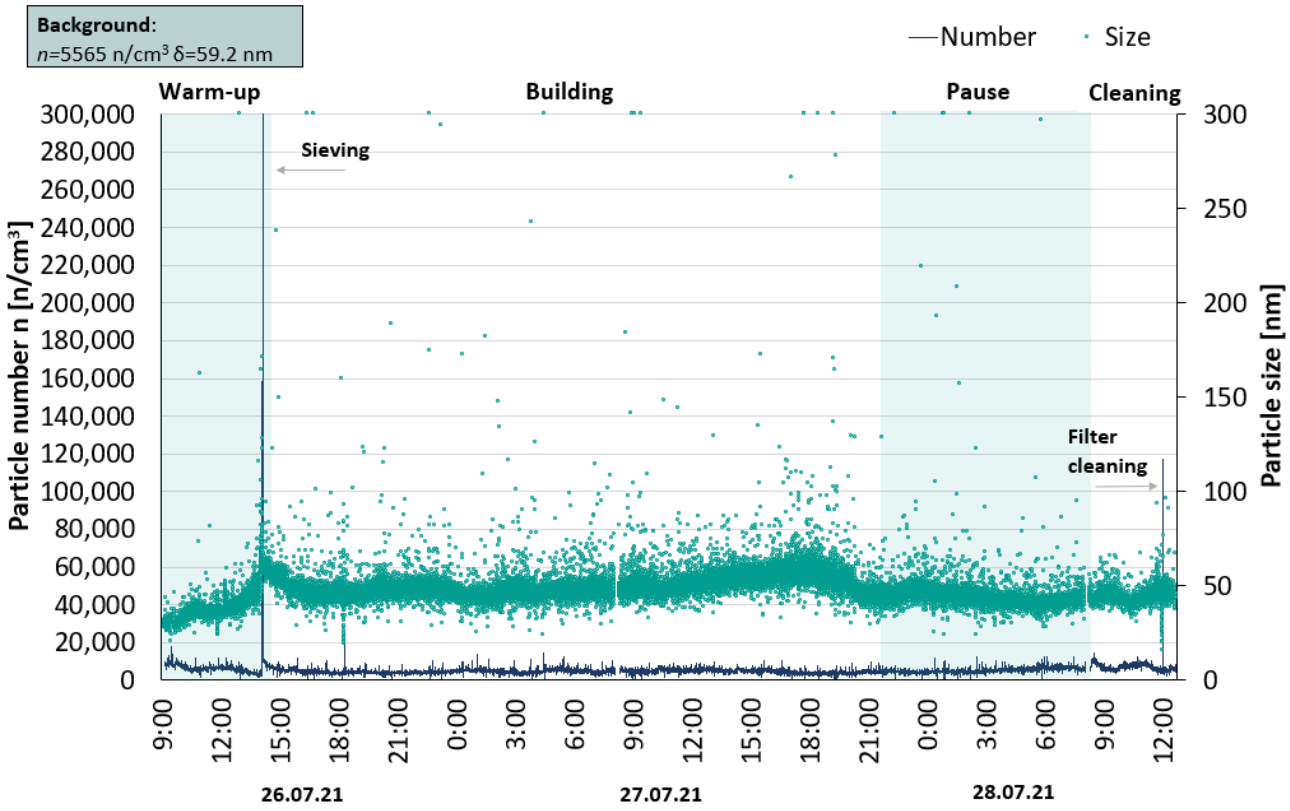

Figure 6. Real-time particle measurement - Environmental monitoring PV_316L_ENV – whole process. Background measurements are displayed at the top left of the chart, confidence interval: number 4805-6326 n/cm^3, size 52.8-63.5 nm.

Figure 6 shows the process PV_316L_ENV, whose particle concentration during building lays below 10,000 n/cm^3. It is possible to highlight a release event during the warmup for 5', where the particle concentration reaches 302,000 n/cm^3 and the average diameter accounts for 170 nm. This peak corresponded to a not-ordinary event during the warmup, i.e., the sieving of the residual powders by the operator.

Personal monitoring confirms the pattern of the environmental one, while the peaks of concentration are higher since the operator interacts directly with the potential sources of NP.

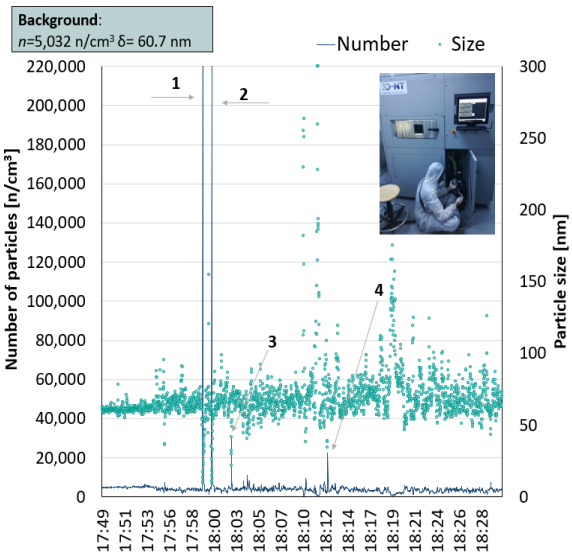

Figure 7. a) Personal monitoring MI_A357_PERS Warmup. Release events: 1. Overflow check (849,400 n/cm^3), 2. Closing overflow door (593,000 n/cm^3), 3. Opening powder container, 4. Charging powders. (background measurements are displayed at the top left of the chart, confidence interval: number 4529-5535 n/cm^3, size 56.4-65 nm).

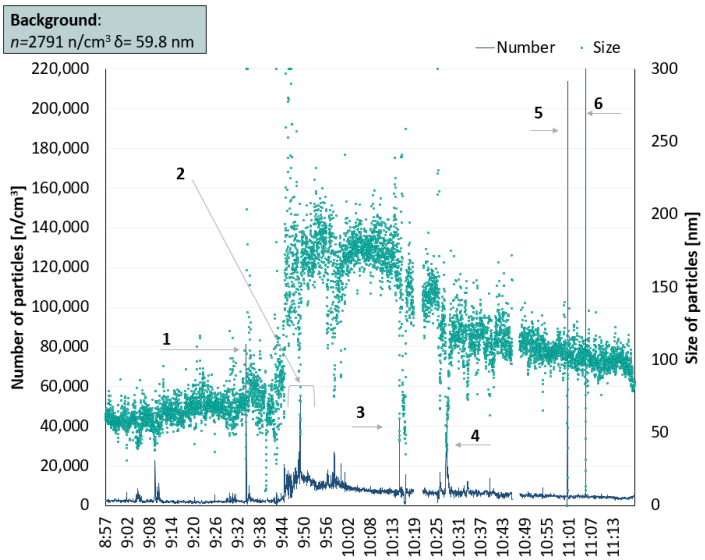

Figure 7. b) Personal monitoring MI_A357_PERS Cleaning Release events: 1. Use of vacuum and cleaning of joints, 2. Cleaning of components of build chamber and moving plate. 3-4. Opening overflow door, 5. Mounting pipe connected to overflow container, 6. Opening filter door. (background measurements are displayed at the top left of the chart, confidence interval: number 2479-3103 n/cm^3, size 52.1-67.5 nm).

The process MI_A357_PERS points out several release events associated to specific activities of the operator. During the warmup (Figure 7a), the main peaks occur in correspondence to not-ordinary events for checking the overflow, i.e., opening and closing of overflow door (respectively 849,000 n/cm^3 and 593,000 n/cm^3). It is important to highlight that this warmup was carried out following the conclusion of a previous process, thus the NP released could have been generated during the former manufacturing. During cleaning (Figure 7b), the release events can be associated to job tasks of the standard workflow: opening and closing of the overflow door (respectively 42,700 n/cm^3 and 47,800 n/cm^3), handling of the overflow pipe and container (213,800 n/cm^3), use of vacuum for cleaning the joints of the build chamber (81,500 n/cm^3) and opening of the filter door (228,000 n/cm^3).

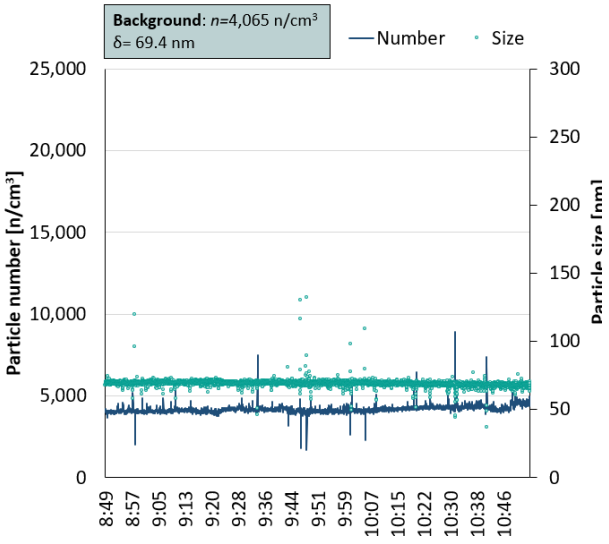

Figure 8. a) MI_Cu_PERS Warm-up. Background measurements are displayed at the top left of the chart, confidence interval: number 3876-4254 n/cm^3, size 67.2-71.6 nm.

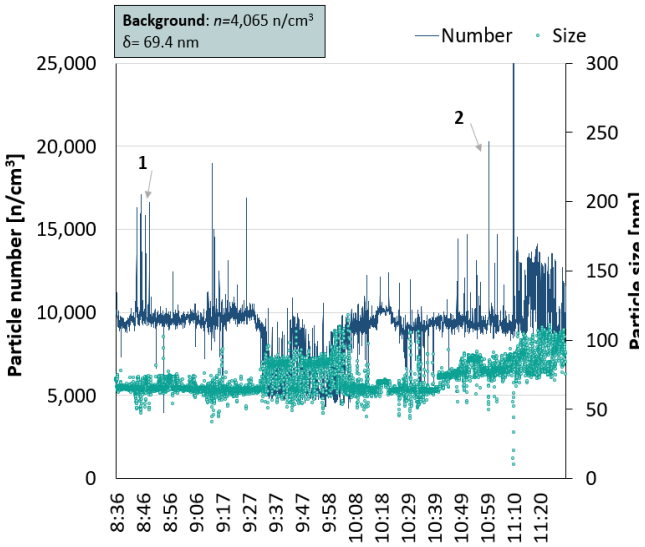

Figure 8. b) MI_Cu_PERS Cleaning. Release events: 1. Cleaning build chamber 2. Cleaning overflow container. Background measurements are displayed at the top left of the chart, confidence interval: number 3876-4254 n/cm^3, size 67.2-71.6 nm.

The monitoring of MI_Cu_PERS presents a reduced release during the warmup (Figure 8a), where the concentration is comparable to the background, while during cleaning (Figure 10b) the release is in general higher than 10,000 n/cm^3. During warmup and cleaning no not-ordinary events (Figure 1) occurred.

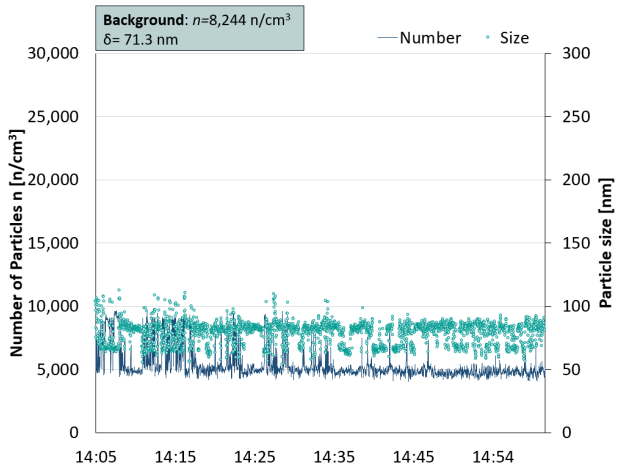

Figure 9. a) PV_316L_PERS warmup. Background measurements are displayed at the top left of the chart, confidence interval: number 5916-10572 n/cm^3, size 52.6-89.9 nm.

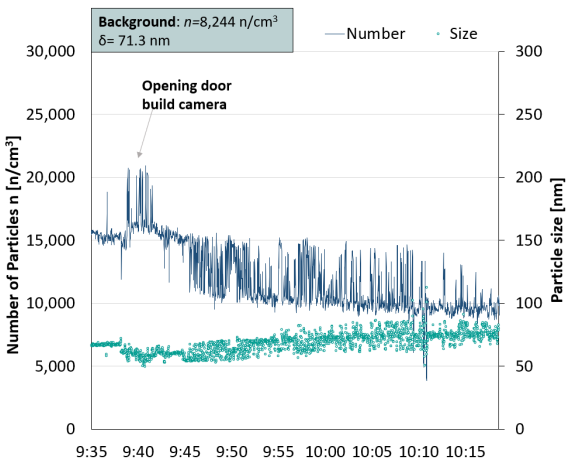

Figure 9. b) PV_316L_PERS cleaning. Background measurements are displayed at the top left of the chart, confidence interval: number 5916-10572 n/cm^3, size 52.6-89.9 nm.

PV_316L_PERS presents a negligible release respect to the background during warmup (Figure 9a), since in this case the process followed the standard workflow, Figure 1, while the monitoring shows higher concentration during cleaning, especially when the operators open the door of the build camera (Figure 9b). The device in UNIPV allows to perform the cleaning initialization with the chamber door closed, limiting the release peaks, in fact the concentration increase when opening the door accounts for additional measurement of around 5000 n/cm^3.

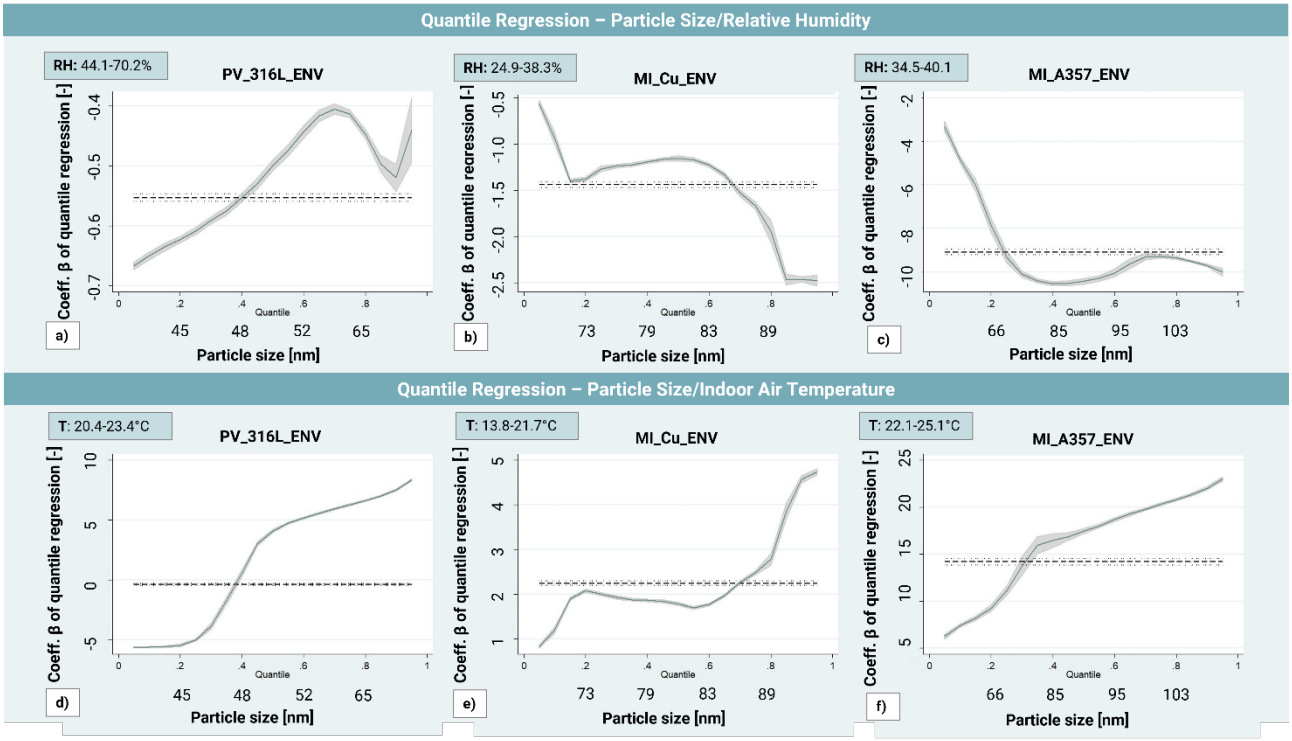

Figure 10. Quantile regression between particle size and relative humidity *RH* (a-c) and indoor air temperature *t* (d-f)

Figure 10 shows the results of the quantile regression between the average size with the relative humidity RH (a-c) and the indoor air temperature T (d-f) calculated as reported in Section 2.3. RH and T are taken as independent variables and are measured in the AM box during the environmental monitoring of the three processes. Median T are similar in all operational phases at UNIPV and during aluminium alloy A357 building at POLIMI, ranging between 21-25 °C, while lower T is measured during pure copper building at POLIMI. Median RH is higher at UNIPV (about 47-60%) compared to POLIMI for both alloys (always lower than 40%).

We can observe negative regression coefficients between the particle size and RH (Figure 10 a-c) and positive regression with the temperature (Figure 10 d-f). This observation is coherent with the inverse correlation generally occurring between HR and T. In PV_316L_ENV (Figure 10a) RH is higher than in MI_Cu_ENV (Figure 10b) and MI_A357_ENV (Figure 10c) (average 46% vs respectively 35% and 31%) and the NP released present a shorter median diameter among the monitored processes (49 nm vs 81 nm and 92 nm). In this case, it is possible to observe an increase of the coefficient of quantile regression from -0.7 to -0.4 for different quantiles (until 0.7) which corresponds to a size interval 10-60 nm, while they reduce at higher quantiles, and thus for particles larger than 60 nm. The decrease of the regression coefficients in the interval 50-70 nm occurs also in the other two processes. In MI_Cu_ENV the regression coefficient curve increases from -0.5 towards -1.5 for particles with diameter lower than 60 nm (about quantile 0.2), become stable in the interval between 70-85 (quantiles 0.2-0.6) and presents a decrease up to -2.5 for larger particles. The trend is comparable also for MI_A357_ENV, although in this case the indices highlight a more significant negative regression coefficients ranging from -3 to -10.5. Between particle size and indoor temperature is observed a positive correlation that increases in parallel to the particle size. The strongest correlation is shown during the process MI_A357_ENV (Figure 10 f), while MI_Cu_ENV presents the weakest one (Figure 12 e).

Discussion

Occupational exposure to metal NP is associated to emerging technologies, and there is still a general lack of structured monitoring data, benchmarks, and reference values. Only provisional limits (nano reference values, NRVs) have been proposed. For powders with density higher than 6,000 kg/m^3, the limit value as weighted average for the working shift is 20,000 particles/cm. For density lower than 6,000 kg/m^3 the limit accounts for 40,000 particles/cm^3. (B. Hendrikx and P. van Broekhuizen, 2013, IFA 2008; SER 2012). Notwithstanding, these limits do not consider exposure peaks that could exceed NRV 10-20 times in several operations and for significant durations, like during building

phase (Figure 5). ACGIH recommends for chemical agents lacking short-term and ceiling TLVs to consider, as benchmark limit values, respectively 3 and five times the average TLV for the working shift. Taking the abovementioned values as reference, although in a low exposure landscape, the monitoring highlighted sudden release events (lasting for around 15-20 seconds) that are associated to specific actions of the operators or activities of the AM devices exceeding 5 times NRVs (ceiling reference). On the other hand, there are no time-intervals highlighting a short-term exposure higher than 3 times NRV for the monitored processes.

Moreover, the monitoring results show the importance of the measurement time-step: the authors adopted one second, the operative standard mode of the monitoring tool. Longer time steps may be unappropriated to describe the dynamics of the nanoparticle release since the observed peaks can be flattened by average values and consequently underestimated (Spinazzè et al., 2016).

In this regard, evaluating the pattern through prolonged monitoring and associating the peaks of release to specific activities is important to adjust the working procedures and to make the operators aware of the potential exposure. The monitoring shows release events correspondence to several actions usually performed during warmup and cleaning, when the operators wear Personal Protection Equipment (PPE).

The presented on-field monitoring identified different release patterns for the used feedstocks. For aluminum A357 alloy and AISI 316L, warmup and cleaning have the highest particle concentration, when the operators use PPE. The highest peaks occur for A357 in correspondence to the specific activities, namely opening overflow door and thanks, cleaning filters, sieving of powders, using of the vacuum. AISI 316L present the lowest number of peaks (during powder sieving, when the operators wear PPE) and reduced release during the process. This material has widely been applied in AM, and it is associated to standard and consolidated process set-up that also ensure controlled release patterns.

A357 is in an advanced research phase and is implemented in industrial setting with proven process parameters. On the other hand, its reduced density represents a significant factor affecting the release of NP, and the highest peaks of concentration among powders are observed. Moreover, the measurement detected further significant peaks in correspondence to the inertization and de-inertization of the build chamber when the operative procedures allow to enter the room without PPE (Figure 3).

Pure copper is not industrially applied as much as stainless steel and aluminium powders because the high reflectivity coupled with high thermal diffusivity makes its L-PBF processability very unstable, resulting in high porosity, oxidation, and poor mechanical properties of the manufactured component (Colopi et al., 2019). The set-up of the parameters for pure copper powder is still an open and ongoing investigation along with the appropriate selection of the laser beam source: green laser or more recently blue lasers (Hori et al., 2021), pulsed wave or continuous wave lasers, single mode or multi-mode/dynamic beam shaping sources are the latest routes to overcame challenges in L-PBF of pure copper. Throughout the experimental activity, the investigation of pure Cu processability was carried out using ultra-high volumetric energy densities (Jiang et al., 2021), which led to a significant vaporization detected during the personal and environmental monitoring phases. The monitored data in Figure 4 highlight that the building phase presents a significant release confirmed also by the additional measurements in Figure 5. The release occurred during the deposition of the first layers at the beginning of the build jobs. Here, the testing of ultra-high energy density conditions likely led to excessive stainless-steel baseplate vaporization along with unproper melting and vaporization of pure Cu powder. The initial process instability was attributed to the scarce number of layers deposited which entailed a direct remelting and vaporization of the baseplate. As shown in Table 1, the energy density necessary for a proper LPBF of stainless-steel powder is two orders of magnitude lower than that tested with pure Cu powder. This witnesses the exposure of the baseplate to vaporization fostered by the process parameters choice. Along with the substrate, pure Cu powder itself is the most sensitive alloy to vaporization with the given process parameters. In fact, as reported in Table 1, pure copper

powder shows the highest estimated vaporization fraction (m') among the treated alloys. Further measurements are needed to better characterize these release events and to improve the safety procedures as well as the features of the AM devices. In fact, during building, no PPE are usually adopted, and the operators may be exposed to a significant number of NP for long time intervals, due to the needed interaction with the AM device for adjusting set-up parameters and restoring the building process. Moreover, these results provide also inputs for the design of the AM devices, introducing new requirements to limit the release of nanoparticles. The sealing of the chamber door needs to be improved to contain the nanoparticles generated by the printing phase, and the filtering of the fumes as well as argon from the building chamber during the de-inertization needs to be adapted for limiting the flows of nanoparticles.

The monitoring campaign confirms that the main NP exposures correspond to several activities that, in the current design of AM devices, are carried out manually: namely handling the powders for charging, cleaning the machine and the environment, and sieving the powders for their re-use. In addition, the monitoring highlights potential risks during the building phase, in case of adjustments by the operators on process parameters. This risk is more significant for research activities working with open-architecture systems on experimental set-up that require process parameters optimization but may occur also in industrial settings in case of malfunctioning or not ordinary events.

The presented measurements deal with three different powders with peculiar toxic profiles. AISI 316L (used at UNIPV) contains cobalt, chromium, and nickel, being the latter carcinogenic by inhalation. The presence of these metals was observed by the authors in POLIMI and UNIPV AM facilities in (Oddone *et al.*, 2021b). The gravimetric techniques applied in that work confirmed the results of previous monitoring in AM working environments (Ljunggren et al., 2019), highlighting to negligible metal concentrations for both inhalable and respirable particles in comparison to available TLVs. Concerning pure copper powder and aluminum A357 alloy (used at POLIMI) no carcinogenic

effects are known, but they are sensitizing agents and can induce asthma, as reported in safety data sheets according to REACH-CLP legislation (European Parliament, 2008).

On the other hand, the evaluation of the toxicity metals at the nanometer scale, that is halfway between classical and quantum physics (Medici et al., 2021), is still in a preliminary research phase, and there is not a complete agreement on the potential health hazard associated to the NP generated as byproducts by AM processes (Wang et al., 2021; Vallabani et al., 2022).

The approach based on gravimetric analysis does not provide a complete characterization of the released powder (Oddone *et al.*, 2021b). The number per unit of air volume, the size and shape of the particles, and the active surface (i.e., the surface area that becomes available for direct interactions with the biological systems) are more significant and increase as the size of the particles decreases (Nanoparticle toxicology, in Casarett and Doull's Toxicology, 2019). As an example, a recent study showed a more intense lung inflammatory reaction in experimental animals when exposed to TiO_2 NP with a 20 nm diameter compared to exposure to 250 nm diameter NP of the same material, while a similar dose- response was observed when, for each of the two particle sizes, the dose was expressed as a surface area (Oberdörster, Oberdörster, and Oberdörster, 2005). Being smaller than single cells and their organelles, exposure to NP can lead to oxidative stress, cellular dysfunction and toxicity, since the human immune system is not suited to recognize and defend against particles smaller than 1 μm (Medici et al., 2021). Moreover, NP could promote macrophages, neutrophils and dendritic cell activation, leading to secretion of proinflammatory cytokines and thus to potential pathologic consequences as lung inflammation and fibrosis (Leikauf, Kim, and Jang, 2020).

Recent Northern European studies, with results similar to ours in terms of concentration and size of metal NP, demonstrated skin and systemic exposure (detected in urine) in a AM facility workers, and consequent alterations in indicators of inflammation and liver function, with normalization after exposure prevention interventions (Ljunggren et al., 2019, 2021; Assenhöj et al., 2021), stressing once again the need for adequate methods of assessment and control of exposure.

According to these considerations, some attempts to systematize with a control banding (CB) qualitative approach, the exposure assessment have been made considering toxicological characteristics of parental materials madding up the powder alloys, the toxicological and dimensional characteristics of NP produced in AM processes and production process features (Sousa et al., 2021). However, the CB approach for qualitative assessment (Zalk, Paik, and Swuste, 2009; Sousa et al., 2019), does not consider the possible dependence of particles concentration and size also on microclimatic parameters. Relative humidity influences the nanoparticle deposition rate, with a significant inverse correlation for particles with a diameter up to 70 nm (Wang et al., 2017). The monitoring in UNIPV and POLIMI confirmed the negative correlation between particle size and relative humidity, whose magnitude is higher for particles smaller than 70 nm (Figure 10, a-c). This observation suggests a potential action of relative humidity in keeping the particles separate, preventing the aggregation mechanism and consequent deposition. Further measurements under different conditions are needed to better assess the role of microclimatic parameters on the particle size and concentration. Nevertheless, the results presented in this work suggest an impact on the potential exposure to NP in AM facilities and thus they deserve to be considered in the risk assessment and controlled during work processes.

Limitations of the study

The results presented in this work deal with a series of alloys and AM devices, with different level of maturity and physical properties, aiming to provide an overview of the nanoparticle release of LPBF. Nevertheless, the monitoring campaign included six processes representing a limited sample characterised by different variables, among all: boundary conditions, operator in charge of managing the activities, length, and complexity of the job. Therefore, the results may be affected by the abovementioned variables, and further measurements including a larger number of processes are needed to provide a consistent overview and reference benchmarks. Moreover, the performed on-field monitoring would require additional measurements to provide a comprehensive chemical

characterization of the nanoparticulate. Nevertheless, some considerations can be based on the identification of the nanoparticle release pattern according to the activities of the operators and process data.

Another limitation of the study lays in the adoption of Testo DiSCMini that allows the implementation of personal monitoring but presents a lower precision than other instruments (e.g., condensation particle counters and scanning mobility particle sizers) and can introduce an error up to ± 30% (Todea et al., 2017). Nevertheless, the main outcomes of the study deal with peaks exceeding the NRV up to 20 times, thus are not affected by the precision of the measure. Further monitoring adopting more accurate measurement devices would allow to validate the results.

Despite these limitations, this work contributes to the characterization of the potential nanoparticle release during LPBF processes and provides preliminary indications for improving the process management and reducing the risks for the operators.

Conclusions and further developments

This study aims to present an overview of the nanoparticle released during AM processes implementing LPBF technology. It deals measurements of considerable length and contributes to describe the particle release with different feedstocks.

The results show a controlled release in the monitored sites, with a limited average exposure of the operators, wearing PPE when the building chamber is open and when handling powders. On the other hand, the prolonged real-time measurements highlight significant peaks of NP concentration corresponding to specific actions. The highest release for AISI 316L and A357 (widely adopted in AM) occurs during warmup and cleaning, where operators wear PPE. Pure copper processes show a significant concentration during building, when operators do not wear PPE. However, pure copper

represents an uncommon powder feedstock in the LPBF framework, whose processability is an ongoing research topic.

These outcomes represent useful inputs to finetune the working procedures and the features of the devices to further improve the level of safety of AM. The potential strategies may rely on introducing higher level of automation for specific operations during cleaning and warmup, increasing the ventilation rate for removing NP in correspondence to the foreseen release events, controlling the temperature and relative humidity to foster the nanoparticle aggregation.

Further monitoring in different sites and conditions are needed to increase the robustness of the results towards the definition of process benchmarks, and release potential of the AM devices with the current technologies.

References

American Conference of Governmental Industrial Hygienists. (2021) TLVs and BEIs. Available at https://portal.acgih.org/s/store#/store/browse/detail/a154W00000BOag7QAD.

Assenhöj M, Ward LJ, Ghafouri B, Graff P, Ljunggren SA. (2021) Metal exposure from additive manufacturing and its effect on the nasal lavage fluid proteome - a pilot study. *PLoS ONE*; **16**: e0256746. p. e0256746.

B. Hendrikx, P. van Broekhuizen. (2013) Nano reference values in the Netherlands. *English version of the article in Gefahrstoffe – Reinhalt Luft*; **10**: 407–14. p. 407–14.

Bengalli R, Gualtieri M, Capasso L, Urani C, Camatini M. (2017) Impact of zinc oxide nanoparticles on an in vitro model of the human air-blood barrier. *Toxicology Letters*; **279**: 22–32. p. 22–32.

Böckin D, Tillman A-M. (2019) Environmental assessment of additive manufacturing in the automotive industry. *Journal of Cleaner Production*; **226**: 977–87. p. 977–87.

Chen R, Yin H, Cole IS, et al. (2020) Exposure, assessment and health hazards of particulate matter in metal additive manufacturing: A review. *Chemosphere*; **259**: 127452. p. 127452.

Colopi M, Demir AG, Caprio L, Previtali B. (2019) Limits and solutions in processing pure Cu via selective laser melting using a high-power single-mode fiber laser. *Int J Adv Manuf Technol*; **104**: 2473–86. p. 2473–86.

Duffin R, Tran L, Brown D, Stone V, Donaldson K. (2007) Proinflammogenic Effects of Low-Toxicity and Metal Nanoparticles In Vivo and In Vitro: Highlighting the Role of Particle Surface Area and Surface Reactivity. *Inhalation Toxicology*; **19**: 849–56. p. 849–56.

European Parliament. (2008) Regulation (EC) No 1272/2008 Classification, labelling and packaging of substances and mixtures, amending and repealing Directives 67/548/EEC and 1999/45/EC, and amending Regulation (EC) No 1907/2006 (Text with EEA relevance). Available at https://eur-lex.europa.eu/legal-content/en/TXT/?uri=CELEX%3A32008R1272.

Fierz M, Houle C, Steigmeier P, Burtscher H. (2011) Design, Calibration, and Field Performance of a Miniature Diffusion Size Classifier. *Aerosol Science and Technology*; **45**: 1–10. p. 1–10.

Fonseca AS, Maragkidou A, Viana M, et al. (2016) Process-generated nanoparticles from ceramic tile sintering: Emissions, exposure and environmental release. *Science of The Total Environment*; **565**: 922–32. p. 922–32.

Hori E, Sato Y, Shibata T, Tojo K, Tsukamoto M. (2021) Development of SLM process using 200 W blue diode laser for pure copper additive manufacturing of high density structure. *Journal of Laser Applications*; **33**: 012008. p. 012008.

ISO standard. (2019) ASTM52921 - 13(2019) Standard Terminology for Additive Manufacturing - Coordinate Systems and Test Methodologies.

Jensen ACØ, Harboe H, Brostrøm A, Jensen KA, Fonseca AS. (2020) Nanoparticle Exposure and Workplace Measurements During Processes Related to 3D Printing of a Metal Object. *Front Public Health*; **8**: 608718. p. 608718.

Jiang Q, Zhang P, Yu Z, et al. (2021) A Review on Additive Manufacturing of Pure Copper. *Coatings*; **11**: 740. p. 740.

Kolb T, Beisser R, Schmidt P, Tremel J, Schmidt M. (2017) Safety in additive manufacturing: Fine dust measurements for a process chain in Laser beam melting of metals. *RTejournal - Forum für Rapid Technologie*; **14**.

Kreyling WG, Hirn S, Möller W, et al. (2014) Air–Blood Barrier Translocation of Tracheally Instilled Gold Nanoparticles Inversely Depends on Particle Size. *ACS Nano*; **8**: 222–33. p. 222–33.

Kuijpers E, Bekker C, Brouwer D, le Feber M, Fransman W. (2017) Understanding workers' exposure: Systematic review and data-analysis of emission potential for NOAA. *Journal of Occupational and Environmental Hygiene*; **14**: 349–59. p. 349–59.

Leikauf GD, Kim S-H, Jang A-S. (2020) Mechanisms of ultrafine particle-induced respiratory health effects. *Exp Mol Med*; **52**: 329–37. p. 329–37.

Ljunggren SA, Karlsson H, Ståhlbom B, et al. (2019) Biomonitoring of Metal Exposure During Additive Manufacturing (3d Printing). *Safety and Health at Work*; **10**: 518–26. p. 518–26.

Ljunggren SA, Karlsson H, Ståhlbom B, et al. (no date) Biomonitoring of Metal Exposure During Additive Manufacturing (3D Printing). 9. p. 9.

Ljunggren SA, Ward LJ, Graff P, Persson A, Lind ML, Karlsson H. (2021) Metal additive manufacturing and possible clinical markers for the monitoring of exposure-related health effects. *PLoS ONE*; **16**: e0248601. p. e0248601.

Medici S, Peana M, Pelucelli A, Zoroddu MA. (2021) An updated overview on metal nanoparticles toxicity. *Seminars in Cancer Biology*; **76**: 17–26. p. 17–26.

Mellin P, Jönsson C, Åkermo M, et al. (2016) Nano-sized by-products from metal 3D printing, composite manufacturing and fabric production. *Journal of Cleaner Production*; **139**: 1224–33. p. 1224–33.

Nanoparticle toxicology, in Casarett and Doull's Toxicology. (2019) , 9th edn. New York: McGraw Hill.

National Institute of Occupational Safety and Health. (2007) Pocket guide to chemical hazards. Available at https://www.cdc.gov/niosh/docs/2005-149/pdfs/2005-149.pdf.

Niaki MK, Torabi SA, Nonino F. (2019) Why manufacturers adopt additive manufacturing technologies: The role of sustainability. *Journal of Cleaner Production*; **222**: 381–92. p. 381–92.

Oberdörster G, Oberdörster E, Oberdörster J. (2005) Nanotoxicology: An Emerging Discipline Evolving from Studies of Ultrafine Particles. *Environmental Health Perspectives*; **113**: 823–39. p. 823–39.

Occupational Safety and Health Administration. (2020) Permissible Exposure Limits. Available at https://www.osha.gov/annotated-pels.

Oddone E, Pernetti R, Fiorentino ML, et al. (2021a) Particle measurements of metal additive manufacturing to assess working occupational exposures: a comparative analysis of selective laser melting, laser metal deposition and hybrid laser metal deposition. *Ind Health*; 2021–0114. p. 2021–0114.

Oddone E, Pernetti R, Fiorentino ML, et al. (2021b) Particle measurements of metal additive manufacturing to assess working occupational exposures: a comparative analysis of selective laser melting, laser metal deposition and hybrid laser metal deposition. *Ind Health*; 2021–0114. p. 2021–0114.

Pieter Van Broekhuize, Wim Van Veelen, Willem-Henk Streekstra, Paul Schulte, Lucas Reijnders. (2012) Exposure Limits for Nanoparticles: Report of an International Workshop on Nano Reference Values. *The Annals of Occupational Hygiene, Volume 56, Issue 5, July 2012, Pages 515–524*; **56,**: 515–24. p. 515–24.

Shi X, Chen R, Huo L, et al. (2015) Evaluation of Nanoparticles Emitted from Printers in a lean Chamber, a Copy Center and Office Rooms: ealth Risks of Indoor Air Quality. *j nanosci nanotechnol*; **15**: 9554–64. p. 9554–64.

Sousa M, Arezes P, Silva F. (2019) Nanomaterials exposure as an occupational risk in metal additive manufacturing. *J Phys: Conf Ser*; **1323**: 012013. p. 012013.

Sousa M, Arezes P, Silva F. (2021) Occupational Exposure to Ultrafine Particles in Metal Additive Manufacturing: A Qualitative and Quantitative Risk Assessment. *IJERPH*; **18**: 9788. p. 9788.

Spinazzè A, Cattaneo A, Limonta M, Bollati V, Bertazzi PA, Cavallo DM. (2016) Titanium dioxide nanoparticles: occupational exposure assessment in the photocatalytic paving production. *J Nanopart Res*; **18**: 151. p. 151.

Steen WM, Mazumder J. (2010) *Laser Material Processing*. London: Springer London. ISBN 978-1-84996-061-8.

Todea AM, Beckmann S, Kaminski H, et al. (2017) Inter-comparison of personal monitors for nanoparticles exposure at workplaces and in the environment. *Science of The Total Environment*; **605–606**: 929–45. p. 929–45.

Vallabani NVS, Alijagic A, Persson A, Odnevall I, Särndahl E, Karlsson HL. (2022) Toxicity evaluation of particles formed during 3D-printing: Cytotoxic, genotoxic, and inflammatory response in lung and macrophage models. *Toxicology*; **467**: 153100. p. 153100.

Wang X, Vallabani NVS, Giboin A, et al. (2021) Bioaccessibility and reactivity of alloy powders used in powder bed fusion additive manufacturing. *Materialia*; **19**: 101196. p. 101196.

Wang Y, Chen L, Chen R, et al. (2017) Effect of relative humidity on the deposition and coagulation of aerosolized SiO2 nanoparticles. *Atmospheric Research*; **194**: 100–8. p. 100–8.

Zalk DM, Paik SY, Swuste P. (2009) Evaluating the Control Banding Nanotool: a qualitative risk assessment method for controlling nanoparticle exposures. *J Nanopart Res*; **11**: 1685–704. p. 1685–704.